Virology 579 (2023) 75–83

Contents lists available at ScienceDirect

Virology

journal homepage: www.elsevier.com/locate/virology

A novel gyrovirus is abundant in yellow-eyed penguin (*Megadyptes antipodes*) chicks with a fatal respiratory disease

Janelle R. Wierenga [a,b], Kerri J. Morgan [b], Stuart Hunter [b], Harry S. Taylor [c,d], Lisa S. Argilla [e], Trudi Webster [f], Jeremy Dubrulle [a], Fátima Jorge [g], Mihnea Bostina [a], Laura Burga [a], Edward C. Holmes [h], Kate McInnes [c], Jemma L. Geoghegan [a,i,*]

[a] Department of Microbiology and Immunology, University of Otago, Dunedin, New Zealand
[b] Wildbase, School of Veterinary Science, Massey University, New Zealand
[c] Biodiversity Group, Department of Conservation Te Papa Atawhai, New Zealand
[d] Diagnostic and Surveillance Services, Biosecurity New Zealand, Ministry for Primary Industries, New Zealand
[e] Wildlife Hospital, Dunedin, Otago Polytechnic School of Veterinary Nursing, New Zealand
[f] Yellow-eyed Penguin Trust, New Zealand
[g] Otago Micro and Nano Imaging, University of Otago, Dunedin, New Zealand
[h] Sydney Institute for Infectious Diseases, School of Medical Sciences, The University of Sydney, Australia
[i] Institute of Environmental Science and Research, Wellington, New Zealand

ARTICLE INFO

Keywords:
Virus
Gyrovirus
Yellow-eyed penguin
Hoiho
Virome
Disease investigation
Avian disease
Conservation

ABSTRACT

Yellow-eyed penguins (*Megadyptes antipodes*), or *hoiho* in te reo Māori, are predicted to become extinct on mainland Aotearoa New Zealand in the next few decades, with infectious disease a significant contributor to their decline. A recent disease phenomenon termed respiratory distress syndrome (RDS) causing lung pathology has been identified in very young chicks. To date, no causative pathogens for RDS have been identified. In 2020 and 2021, the number of chick deaths from suspected RDS increased four- and five-fold, respectively, causing mass mortality with an estimated mortality rate of >90%. We aimed to identify possible pathogens responsible for RDS disease impacting these critically endangered yellow-eyed penguins. Total RNA was extracted from tissue samples collected during post-mortem of 43 dead chicks and subject to metatranscriptomic sequencing and histological examination. From these data we identified a novel and highly abundant gyrovirus (*Anelloviridae*) in 80% of tissue samples. This virus was most closely related to *Gyrovirus 8* discovered in a diseased seabird, while other members of the genus *Gyrovirus* include *Chicken anaemia virus*, which causes severe disease in juvenile chickens. No other exogenous viral transcripts were identified in these tissues. Due to the high relative abundance of viral reads and its high prevalence in diseased animals, it is likely that this novel gyrovirus is associated with RDS in yellow-eyed penguin chicks.

1. Introduction

Yellow-eyed penguins (*Megadyptes antipodes*), or *hoiho* in te reo Māori, are a critically endangered species endemic to Aotearoa New Zealand and considered one of the rarest penguins in the world. There are two populations of yellow-eyed penguins: northern (occupying mainland New Zealand and Stewart Island/Rakiura plus adjacent islands) and southern (on subantarctic Auckland Islands and Campbell Island). The northern population has experienced a dramatic decline with numbers decreasing by 75% over the past 30 years. Due to this decline, it is speculated that yellow-eyed penguins will become extinct from the mainland of New Zealand within the next two decades (Mattern et al., 2017).

Infectious diseases affecting young chicks are one of the major threats to the extinction of yellow-eyed penguins. Diphtheritic stomatitis associated with *Corynebacterium* spp. has caused significant mortality since its emergence in 2002, with one study reporting the disease in 50% of chicks examined post-mortem (Alley et al., 2017). Although its role in chick mortality is unclear, *Leucocytozoon* spp. have been reported at a high prevalence and causing mortality in both mainland and

* Corresponding author. Department of Microbiology and Immunology, University of Otago, Dunedin, New Zealand.
E-mail address: jemma.geoghegan@otago.ac.nz (J.L. Geoghegan).

https://doi.org/10.1016/j.virol.2022.12.012
Received 28 October 2022; Received in revised form 12 December 2022; Accepted 23 December 2022
Available online 2 January 2023

subantarctic populations (Argilla et al., 2013). Another disease, termed respiratory distress syndrome (RDS), was initially identified in 2019, although historical epidemiological records show the first suspected cases as early as 2015. This manifests as lung congestion and haemorrhage along with lymphoid depletion in the spleen and bursa (unpublished). In 2020 and 2021, the number of chick deaths from RDS increased four- and five-fold compared to 2019, respectively, with a mortality rate of over 90%, and chicks typically succumbed to the disease within the first week of life.

We used a metatranscriptomic approach to identify possible causative agents associated with RDS in yellow-eyed penguins. This led to the discovery of a novel and highly abundant gyrovirus. Gyroviruses are small, non-enveloped DNA viruses within the family *Anelloviridae*, initially characterised as circoviruses but reclassified into the family in 2017 (Rosario et al., 2017; Kraberger et al., 2021). Currently classified gyroviruses possess negative-sense, single-stranded DNA circular genomes of approximately 2000–2400 nucleotides in length. Gyroviruses utilise the host machinery for replication and have three overlapping viral protein (VP) open-reading frames: VP1, which encodes the viral capsid; VP2; and VP3.

Gyroviruses are known to cause disease in avian hosts, while additional viral species have been identified from the faeces of domestic cats (Niu et al., 2019), mice (Fang et al., 2017), ferrets (Feher et al., 2015), dogs (Liu et al., 2022) and humans (Phan et al., 2015). The best-known virus in this genus is *Chicken anaemia virus*, which causes anaemia, poor growth and severe immunosuppression in young chicks (Noteborn et al., 1994; Smyth et al., 1993; Yuasa et al., 1979; Goryo et al., 1985). *Chicken anaemia virus* is found worldwide and causes significant mortality among chicks not protected by maternal antibodies. Other gyroviruses have been identified in diseased avian hosts, including in seabirds (Li et al., 2015; Waits et al., 2018; Goldberg et al., 2018; Truchado et al., 2019; Feher et al., 2022). Herein, we describe a new gyrovirus associated with RDS in yellow-eyed penguins.

2. Results

2.1. Disease investigation, histology and electron microscopy

Yellow-eyed penguin chicks that died with suspected RDS during the November to December 2021 hatching season across eastern Otago, New Zealand were investigated to identify the possible causative agent of the disease. These chicks typically died within the first week of life with ages ranging between two and 10 days old (median = five days). A total of 43 penguin chicks underwent post-mortem examination within 1–2 days of death after showing possible signs of RDS.

From a total of 137 wild yellow-eyed penguin chicks that were admitted to the Dunedin Wildlife Hospital during the 2021 breeding season, 31 (22.6%) that presented between 3–19 November demonstrated clinical evidence of respiratory disease within their first week of life. The majority of these birds died (n = 24, 77%) or were euthanised (n = 3, 10%) within 12–24 h of presentation, with one bird (3%) surviving for 5 days with intensive veterinary support before succumbing. Three (10%) birds were successfully treated and were returned to the nest.

In most cases, the clinical progression of respiratory disease was very rapid. Generally, affected birds demonstrated a progressive increase in respiratory rate and effort, and as the disease progressed, birds became very weak and often recumbent, with pale mucous membranes and evidence of hypothermia despite the provision of external heat. Terminally, chicks presented with coelomic distension, presumably due to overinflation of airsacs as a result of agonal gasping, and birds were visibly cyanotic with a reduced level of consciousness. In addition to the 28 birds that died in hospital, one died enroute to hospital, one was euthanised due to a limb deformity and a further 13 neonates died at the nest during this same period (total n = 43).

Gross post-mortem examination identified abnormal lung tissue bilaterally in 88% (38/43) of chicks, characterised as dark pink to dark purple lungs with obvious haemorrhage and clots within the lungs. A consistent histopathological finding was the presence of proteinaceous fluid (Fig. 1a, red box) and haemorrhage (Fig. 1a, yellow box) within the parabronchi combined with partial or full collapse of the smaller airways, the atria and air-capillaries (Fig. 1). Epithelial cells lining the atria and air-capillaries were often hyperplastic and hypertrophic and there were small numbers of macrophages within these airways. Generalised congestion as well as oedema of interlobular septae was also a consistent feature. Within the spleen and bursa, there was lymphoid depletion as well as evidence of active lympholysis.

Yellow-eyed penguin chicks (n = 9) were characterised as 'RDS suspected' when they had clinical signs associated with respiratory disease prior to death and/or upon gross post-mortem the lungs were characterised as dark pink to purple in colour with or without clots in the lung tissue upon extraction. Chicks (n = 31) were characterised as 'RDS confirmed' based on histopathological analyses as described above. Similarly, chicks (n = 3) were characterised as 'RDS not suspected' based upon histopathological analyses of the tissues. Of the three chicks without RDS, the cause of death for two were consistent with aspiration pneumonia at 10 and 11 days of age; while the cause of death for the remaining chick (15 days of age at time of death) was unknown.

Electron microscopy investigation of the diseased lung and spleen tissue demonstrated extended cytopathic effect in all the specimens (Supplementary Figs. 1 and 2). This included large vacuoles, swollen mitochondria, and nuclear fragmentation with chromatin aggregates close to the nuclear rim. Notably, cells in the spleen sample showed characteristic electron dense rings in the nuclei similar to that reported for *Chicken anaemia virus* (Jeurissen et al., 1992).

2.2. Viral diversity and abundance

Metatranscriptomic sequencing of multiple tissue samples (bursa, kidney, liver, lung, spleen) from each individual yielded sequencing libraries containing between 44.5 and 85.1 million paired-end reads that were *de novo* assembled into 231,069–964,934 contigs (Fig. 1). Forty-three libraries were evaluated for viral transcripts likely infecting eukaryotic hosts (excluding plant, fungi and protists). A sequence similarity-based search for exogenous viruses identified viral transcripts as a novel gyrovirus (*Anelloviridae*) in 34 of the 43 samples (79%), tentatively named yellow-eyed penguin gyrovirus. No other exogenous viral transcripts were identified. Of those samples with suspected and confirmed RDS, gyrovirus was identified in 32 of 40 (80%) at standardised abundances ranging from 7×10^{-7} to 0.00015, comparable to other avian viral abundances found in penguins (Chapman et al., 2016) (Fig. 2, Supplementary Table 1). Two out of three samples that were not suspected of having RDS upon gross post-mortem also contained gyrovirus sequencing reads at similar abundances, although this could reflect subjective aspects of disease diagnosis (see Discussion).

2.3. PCR confirmation of yellow-eyed penguin gyrovirus

PCR was performed to confirm and identify the presence of yellow-eyed penguin gyrovirus from the same tissue samples as used for the metatranscriptomic sequencing (Fig. 2). The PCR was confirmed and optimised on two samples that had confirmed RDS status upon histopathological examination and high relative abundances of yellow-eyed penguin gyrovirus sequencing reads. PCR was then performed on all samples as individual tissues (including bursa, kidney, liver, lung and spleen). Three samples that tested positive upon PCR for yellow-eyed penguin gyrovirus and were suspected or confirmed as RDS had no gyrovirus sequencing reads (Fig. 2). PCR results largely agreed with the presence or absence of yellow-eyed penguin gyrovirus in the pooled RNA sequencing results. Where discrepancies occurred, for example those samples that were PCR positive, but no virus reads were detected, were likely due to the pooled RNA obtained from all tissue samples

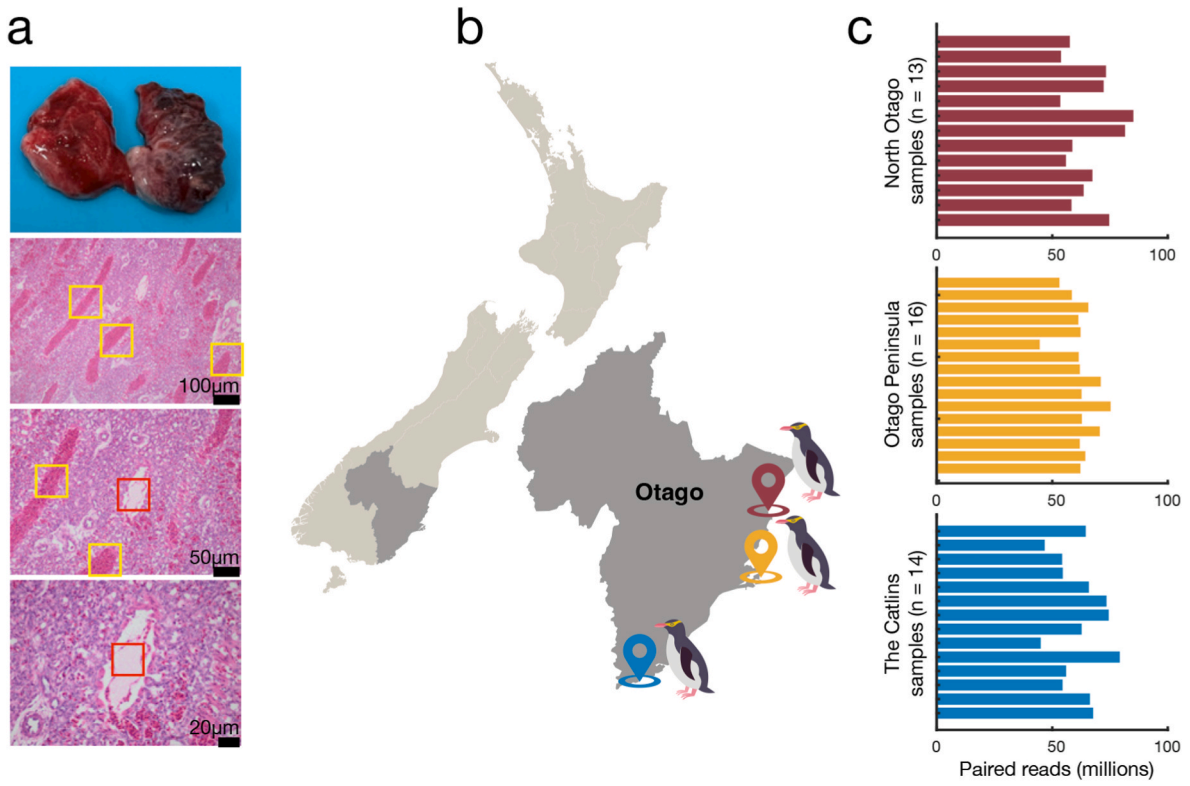

Fig. 1. (a) Fresh lung tissue (top) and lung histology from a yellow-eyed penguin (*Megadyptes antipodes)* chick that was diagnosed with respiratory distress syndrome (RDS); yellow boxes: blood within parabronchi, red boxes: proteinaceous fluid within parabronchi. (b) Sampling locations of yellow-eyed penguin chicks across the east coast of Otago, New Zealand (north Otago = red; Otago peninsula = yellow; The Catlins = blue). (c) Total number of paired-end RNA sequencing reads obtained from yellow-eyed penguin chick tissue samples with ribosomal RNA depletion.

diluting the overall RNA in the sample coupled with high sensitivity of PCR.

2.4. Genome organisation and phylogenetic characterisation of a novel gyrovirus

A total of 29 full and a further five partial genomes of the novel virus were assembled *de novo* from the 43 samples, which all shared >95% nucleotide sequence identity. The novel yellow-eyed penguin gyrovirus genome contained 2610 nucleotides, the largest known gyrovirus genome, and three overlapping open reading frames: VP1, VP2 and VP3 (Fig. 3). Both VP1 and VP2 shared 41% and 27% amino acid identity, respectively, to its closest relative, *Gyrovirus 8*, identified in a diseased northern fulmar (*Fulmarus glacialis*) sampled from California (Li et al., 2015). In contrast, VP3 did not share sequence homology to any other known protein, as is often the case with this ORF in other gyroviruses. The VP1 of the yellow-eyed gyrovirus contained the signature 'WW [R/N]W[S/A]' motif at position 153 with an arginine-rich N-terminus region, while the VP2 contained the conserved 'WX7HX3CXCX5H' motif at residue 96 (Fig. 3).

To infer the evolutionary history of yellow-eyed penguin gyrovirus, we estimated phylogenetic trees for both VP1 and VP2 among other known gyroviruses using *Torque teno virus 1* (NP_817122.1), a non-gyrovirus member of the *Anelloviridae*, as an outgroup (Fig. 3). Within VP1, yellow-eyed gyrovirus clustered with *Gyrovirus 8*, which caused disease in the northern fulmar, while VP2 fell within a clade of gyroviruses infecting seabirds, including *Ashy storm-petrel gyrovirus* (Waits et al., 2018).

We next inferred the phylogeography of all full and partial yellow-eyed gyrovirus genomes obtained (34 of 43 samples) across the three sampling sites (Fig. 4). All genomes fell across two distinct genomic clades (termed A and B), that showed little spatial structure with all three sampling locations contained in both clades. We also found no clustering by gross or confirmed post-mortem RDS status.

2.5. Total infectome characterisation

RNA sequencing data were further evaluated for the presence of bacterial, protozoal and fungal organisms (Fig. 5). The *Enterobacteriaceae*, *Enterococcaceae* and *Staphylococcaceae* families were consistently the most abundant and prevalent across samples while *Aspergillus* spp. were the most abundant fungi detected. Transcripts identified as *Plasmodiaaceae* were found in very few of the libraries in low abundances. It is worth noting, however, that taxonomic misassignment of host genes to microbial organisms is commonplace.

3. Discussion

Our metatranscriptomic investigation into the possible causative agents of the highly fatal respiratory disease syndrome (RDS) affecting yellow-eyed penguin chicks revealed a novel, divergent and highly abundant gyrovirus within the *Anelloviridae*, tentatively named yellow-eyed penguin gyrovirus. This novel gyrovirus was most closely related to *Gyrovirus 8* found in a diseased northern fulmar (Li et al., 2015). Other viruses within the genus *Gyrovirus* are known to infect avian species and cause similar pathology. In particular, *Chicken anaemia virus* is a well-characterised pathogenic virus in the *Anelloviridae* causing anaemia, haemorrhage and immunosuppression in poultry chicks, inflicting significant economic losses to the industry (Yuasa et al., 1979; Goryo et al., 1989; Stanislawek and Howell, 1994; McNulty et al., 1989). *Chicken anaemia virus* can be transmitted both horizontally and vertically and, as a small circular DNA virus, is relatively stable and resistant to most disinfectants (Yuasa et al., 1979; Yuasa, 1992; Welch et al., 2006; Urlings et al., 1993).

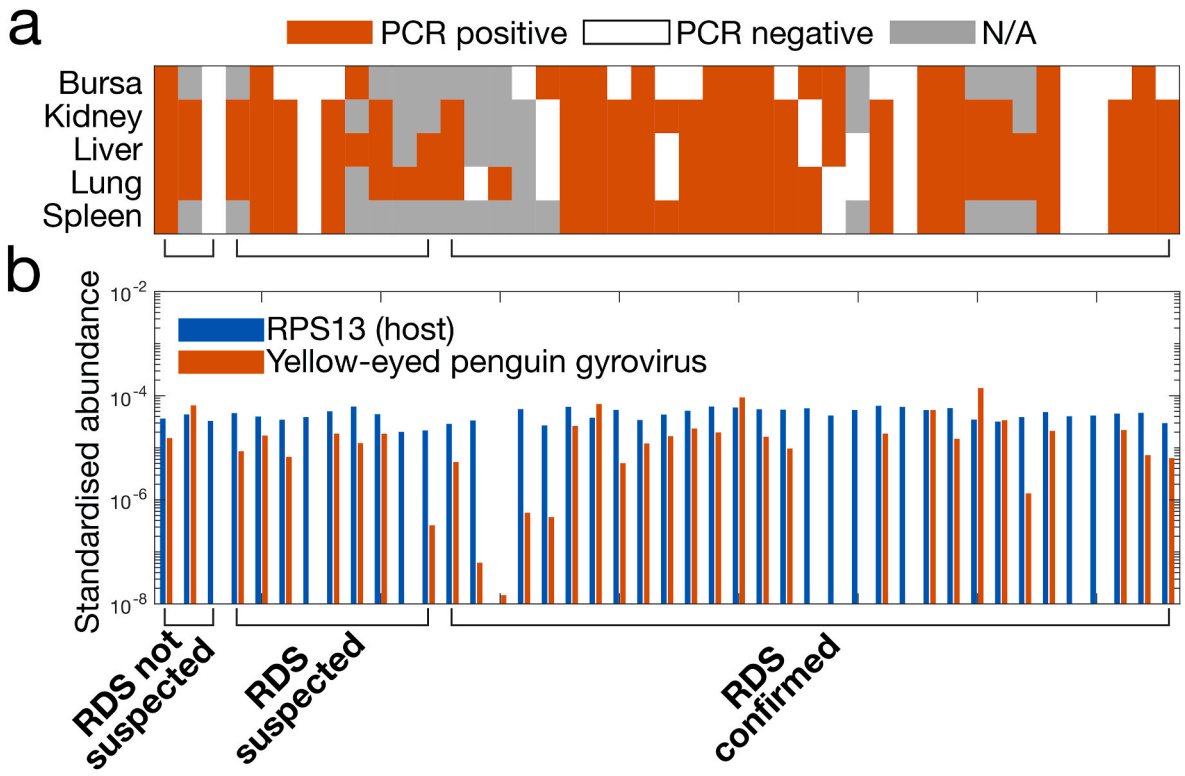

Fig. 2. (a) Tissue samples collected from deceased yellow-eyed penguin chicks (*Megadyptes antipodes*) during the 2021 breeding season that were PCR positive for a novel yellow-eyed penguin gyrovirus (red), PCR negative (white) or not collected (or exhausted) (grey) across five different tissue samples. (b) Standardised relative abundances of the pooled RNA sequencing libraries of a host gene, ribosomal protein s13 (RPS13) (blue) and yellow-eyed penguin gyrovirus (red) across samples that were deemed: (i) respiratory disease syndrome (RDS) not suspected; (ii) RDS suspected at gross post-mortem; and (iii) RDS confirmed with histology.

Phylogenetic analysis of full and partial yellow-eyed penguin gyrovirus genomes identified two distinct clades with little spatial structure among sampling locations and no clustering with gross post-mortem RDS status. The relatively high diversity among yellow-eyed penguin gyrovirus genomes suggested sustained transmission of the virus in the population, compatible with outbreaks dating to at least 2015 when the disease was first identified during post-mortem examination. Further testing and genome sequencing of historical samples suspected of RDS will help to elucidate the evolutionary history of this novel virus.

RDS in yellow-eyed penguin chicks is a recently identified disease causing high mortality despite intensive veterinary intervention. During the 2020 and 2021 seasons, 15% and 23% of the chicks that were monitored on the mainland died as a result of RDS, respectively. Although clinical symptoms are highly suggestive, there are a number of potential causes of respiratory disease in young penguins (Alley et al., 2017; Thijl Vanstreels et al., 2016; Gartrell et al., 2017; Gill and Darby, 1993; Wuenschmann et al., 2006). At present, RDS is highly suspected on post-mortem with grossly visible dark pink to purple lungs with extensive haemorrhage identifiable on cut surface and histological examination provides further confirmation. As a consequence, we developed a PCR test for yellow-eyed penguin gyrovirus that can be used in future breeding seasons to understand the true prevalence of the virus among both diseased and healthy populations.

We attempted to identify other potential causative pathogens of bacterial, protozoal or fungal origin. The majority of bacterial organisms identified were likely typical commensal flora rather than pathogens. In addition, it is likely that much of the bacterial growth occurred post-mortem: dead chicks were in warm environments either in hospital incubators or under the parent in the nest, which could have promoted growth of bacteria in tissue that is normally sterile. Further, contamination during gross post-mortem from the gastrointestinal tract was also possible.

A few samples that tested positive upon PCR for yellow-eyed gyrovirus contained no gyrovirus sequencing reads. In addition, several samples that were confirmed or suspected RDS had an absence of gyrovirus reads. Nevertheless, the range of possible disease phenotypes for RDS is not well understood and gross post-mortem is highly subjective. In addition, there were inconsistencies of tissue types collected across individuals as well as possible tissue decomposition that would likely affect nucleic acid extraction. Finally, pooled RNA from across the five tissue types collected in most cases likely diluted viral RNA that was present in only small abundances and/or in few tissues.

Overall, both the prevalence and relatively high abundance of yellow-eyed gyrovirus supports the pathogenic potential of this virus. In addition, the absence of other exogenous viral transcripts and other known pathogenic microbes suggests that yellow-eyed penguin gyrovirus is likely associated with RDS. However, further work is necessary to confirm this association, to fully exclude yellow-eyed gyrovirus as an opportunistic secondary infection or that a secondary, unidentified infection is responsible for RDS, and to better understand the characteristics of this disease (e.g. transmission) to enable appropriate management recommendations.

4. Materials & methods

4.1. Ethics

This study was conducted under animal ethics approval MUAEC Protocol 21/42 from Massey University and the New Zealand Department of Conservation Permit Authorisation Number 94843-FAU and 94902-FAU.

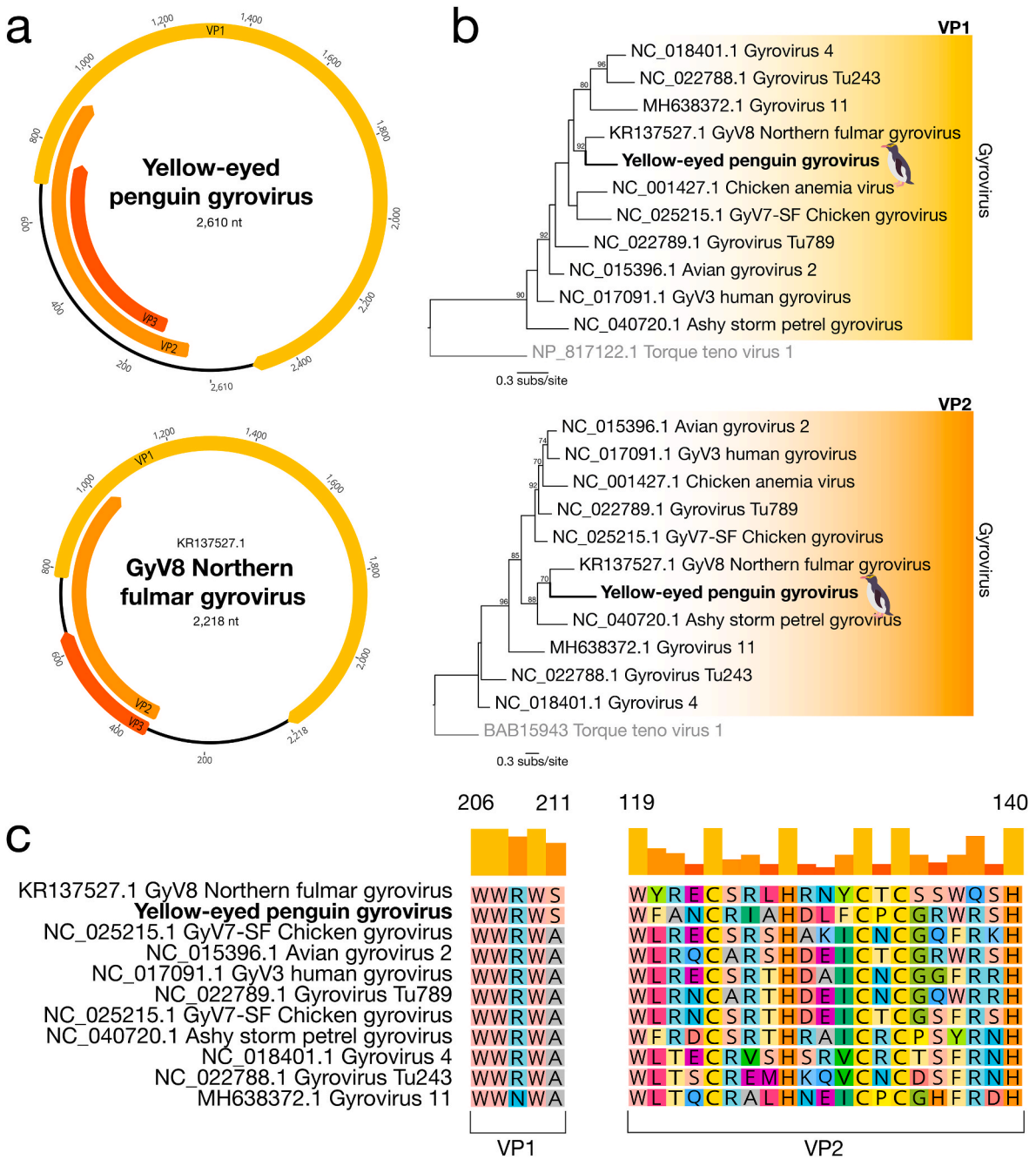

Fig. 3. (a) Genome structure of yellow-eyed penguin gyrovirus (top) illustrating a monopartite, circular, ssDNA genome containing 2610 nucleotides, in comparison with Gyrovirus 8 identified in a northern fulmar (*Fulmarus glacialis*) from California (lower). The positions of viral proteins (VP) 1, 2 and 3 are shown. (b) Maximum likelihood phylogenetic trees of VP1 (top) and VP2 (lower) of viruses within the Gyrovirus genus using Torque teno virus 1 as an outgroup. The topological position of yellow-eyed penguin gyrovirus is shown in bold. Branches are scaled to the number of amino acid substitutions per site. Node support of >70% is shown. (c) Signature conserved motifs within VP1 and VP2 across members of the Gyrovirus genus.

4.2. Sample collection and post-mortem

Three populations of yellow-eyed penguins are monitored annually by the New Zealand Department of Conservation along with various organisations from three regions across Otago, New Zealand. Samples collected in this study originated from Moeraki, North Otago (GPS -45° 21′ 59.99" S,170° 50′ 59.99" E; n = 13), Otago Peninsula (−45° 51′ 17.99" S, 170° 38′ 59.99" E; n = 16) and The Catlins (−46° 29′ 59.99" S, 169° 29′ 59.99" E; n = 14) during the November and December 2021 breeding season (Fig. 1). Newly hatched chicks were monitored and weighed every two to three days and chicks from nests that demonstrated respiratory symptoms or weight loss were immediately transferred to the Dunedin Wildlife Hospital for veterinary treatment.

Affected chicks were immediately placed in incubators set at 32 °C (34–35 °C for those with hypothermia) flooded with 100% oxygen. Lactated Ringer's solution was administered subcutaneously (100 ml/kg/day) and broad spectrum anti-microbials were initiated including 100 mg/kg amoxyclav (400 mg amoxycillin and clavulanic acid 57 mg) PO BID; 15 mg/kg enrofloxacin PO BID and 5 mg/kg voriconazole PO SID-BID. Meloxicam (5 mg/kg PO) was provided once birds were rehydrated. As chicks generally presented with ileus due to being hypothermic and clinically unwell, food was withheld until chicks

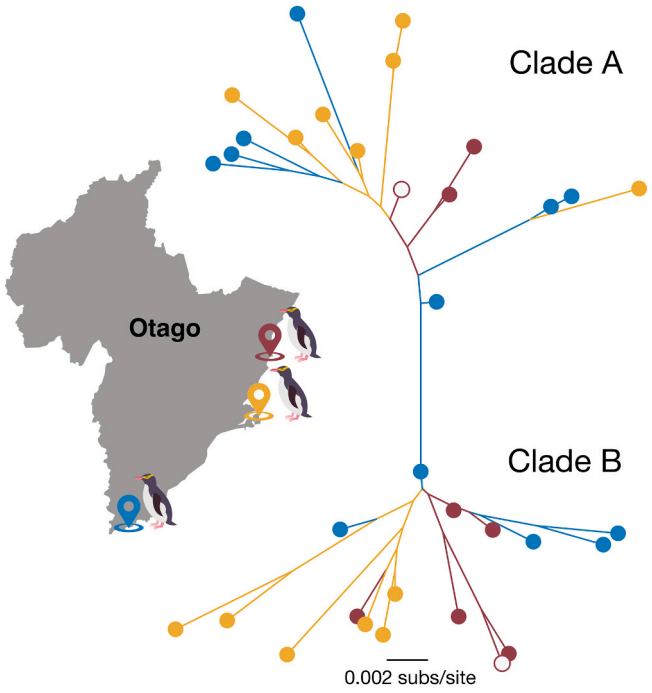

Fig. 4. Unrooted maximum likelihood phylogenetic tree of the full (n = 29) or partial (n = 5) genomes of yellow-eyed penguin gyrovirus identified from multiple breeding sites on mainland New Zealand in organ tissue metatranscriptomes. Branches are scaled to the number of nucleotide substitutions per site. Branches and tips are coloured to illustrate the sampling site shown on the adjacent map. Those samples that, upon post-mortem, were not suspected of having RDS are illustrated as unfilled circles. All samples fell within two major clades, annotated A and B.

clinically stabilised, after which fish slurry was provided via gavage up to five times daily as tolerated.

Neonatal yellow-eyed penguin chicks that died during this period had gross post-mortem examinations performed by a veterinarian within 24 h of death, with dead chicks placed in a refrigerator at 4 °C prior to examination. Tissues that were collected included brain, entire gastrointestinal tract including the oral cavity, lung, heart, thyroid glands, liver, spleen, bursa of Fabricius, adrenal glands, kidneys, yolk sac (if present) and skeletal muscle, although not all tissues were collected for all individuals (see Supplementary Table 1). In situations of marked decomposition of the body either the lung tissue, as this was the observable abnormal tissue that could still be evaluated grossly, or the lung, liver and kidney tissue were collected for analysis; however, in most cases, lung, liver, kidney, bursa of Fabricus and spleen were utilised. Tissues were stored in sterile vials in RNAlater® as well as in 10% formalin for histopathological analyses. Tissues in RNAlater® were immediately stored in a −80 °C freezer.

4.3. Histology

Formalin fixed tissue samples from 34 chicks (out of 43 total) were embedded in paraffin and 4-μm thick sections were stained with hematoxylin and eosin for histological examination. Tissues were examined for the presence of proteinaceous fluid and haemorrhage within the parabronchi combined with partial or full collapse of the smaller airways, the atria and air-capillaries in the lungs.

4.4. Electron microscopy

Initially small lung tissue fragments collected during post mortem examination were fixed in freshly prepared 2% glutaraldehyde in 0.1 M cacodylate buffer pH7.4 for at least 24 h. Following identification of yellow-eyed penguin gyrovirus by metatranscriptomic sequencing in most tissue samples, spleen samples also collected during necropsy and stored at −80 °C were thawed and fixed as described above. The following steps were performed at room temperature under agitation. After primary fixation, tissues were washed three times for 10 min with 0.1 M cacodylate buffer and post-fixed in 2% osmium tetroxide in 0.1 M cacodylate buffer for 1 h. Specimens were then washed three times for 10 min with 0.1 M cacodylate buffer, then twice with doubled distilled water for 10 min followed by dehydration through a series of ascending grades of ethanol concentrations (50%, 70% and 95%, and 2 × 100% for 10 min each, and finally 100% for 20 min), and rinsed twice with propylene oxide for 15 min. The propylene oxide was replaced by dilution of Suprr's resin in propylene oxide (1:1 propylene oxide:resin for 20 min and 1:2 propylene oxide:resin for 40 min). Tissue samples transitioned through three Spurr's resin changes with 4-h incubation time. Each fragment was then transferred to an embedding mould with fresh resin and polymerised for 48 h at 60 °C. Ultrathin sectioning (85 nm) was done with a diamond knife on a Leica EM UC7 ultramicrotome and collected on formvar-coated copper slot grids. Sections were stained with uranyl acetate and lead citrate and investigated using a Philips CM100 transmission electron microscope (TEM).

4.5. RNA extraction and sequencing

Frozen tissue was partially thawed and submerged in lysis buffer containing 1% β-mercaptoethanol and 0.5% Reagent DX (Qiagen) before tissues were homogenised together with TissueRupture (Qiagen). The homogenate was centrifuged to remove any potential tissue residues, and RNA from the clear supernatant was extracted using the Qiagen RNeasy Plus Mini Kit. RNA was quantified using NanoDrop (ThermoFisher) and RNA from each tissue type was pooled into one sample per individual. Extracted RNA was subject to total RNA sequencing. Libraries were prepared using the Illumina Stranded Total RNA Prep with Ribo-Zero Plus (Illumina). Paired-end 150bp sequencing of the RNA libraries was performed on the Illumina NovaSeq 6000 platform (S4 300 lane).

4.6. Virome composition analysis

Sequencing reads were first quality trimmed then assembled *de novo* using Trinity RNA-Seq (Haas et al., 2013). The assembled contigs were annotated based on similarity searches against the NCBI nucleotide (nt) and non-redundant protein (nr) databases using BLASTn and Diamond (BLASTX) (Buchfink et al., 2015), and an e-value threshold of 1×10^{-5} was used as a cut-off to identify positive matches. We removed non-viral hits including host contigs with similarity to viral sequences (e.g. endogenous viral elements). To reduce the risk of incorrect assignment of viruses to a given library due to index-hoping, those viruses with a read count less than 0.1% of the highest count for that virus among the other libraries were assumed to be contaminated.

4.7. Virus abundance and diversity

Viral abundance was estimated using Trinity with the "align and estimate abundance" tool. The method of abundance estimation used was RNA-Seq by Expectation-Maximisation (RSEM) (Li and Dewey, 2011) and the alignment method used was Bowtie2 with "prep_reference" flag enabled (Langmead and Salzberg, 2012). Estimated viral abundances were first standardised against the number of raw reads in each library and then compared to standardised abundances of ribosomal protein s13 (RPS13), which is stably expressed in avian hosts (Chapman et al., 2016). Putative eukaryotic-associated viral transcripts were confirmed by translating open reading frames (ORFs) on Geneious Prime (v. 2022.2.1) and checked via BLASTp (https://www.geneious.com) (Altschul et al., 1990). Viruses were categorised based on viral family and considered novel viruses if they shared <90% amino acid

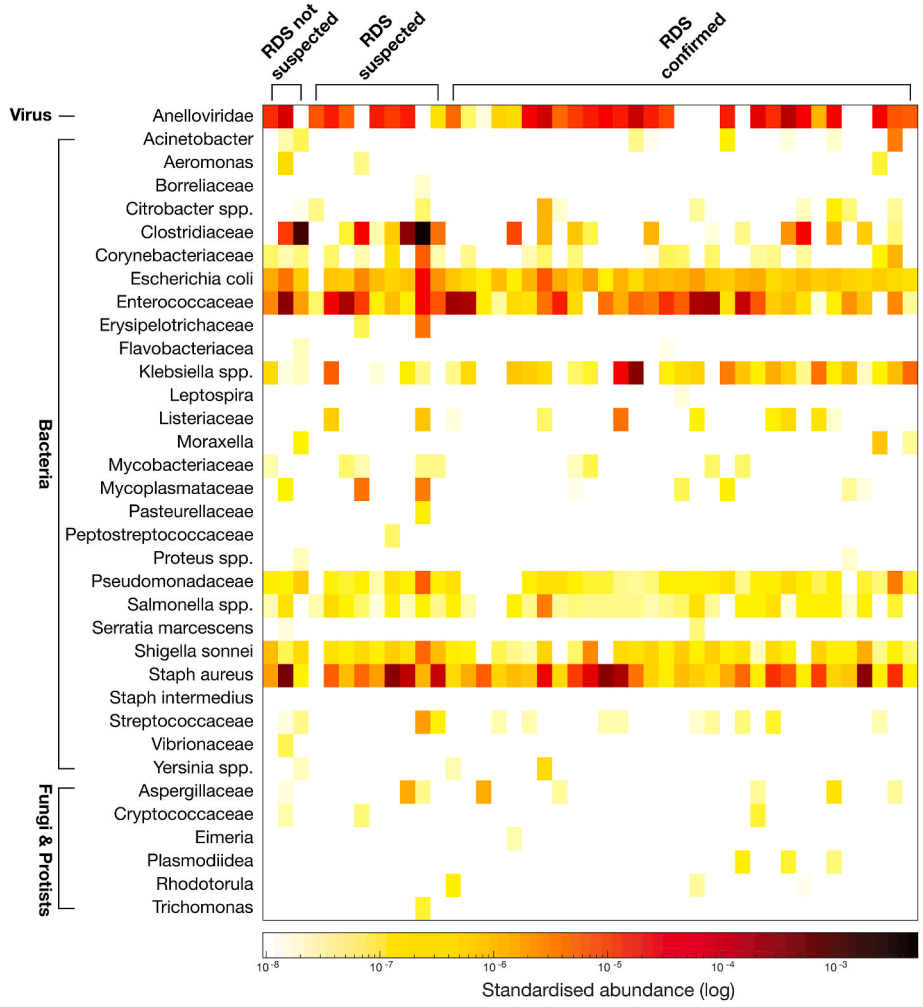

Fig. 5. Standardised read abundance of viral, bacteria, fungi and protist families/genera detected through metatranscriptomic sequencing of tissues from deceased yellow-eyed penguin (*Megadyptes antipodes*) chicks (n = 43) across samples that were deemed: (i) respiratory disease syndrome (RDS) not suspected; (ii) RDS suspected at gross post-mortem; and (iii) RDS confirmed with histology.

similarity within conserved regions (polymerase, viral protein (VP) regions) to known viruses.

4.8. Virus phylogenetic characterisation

To infer the evolutionary relationships of virus transcripts identified, viral contigs were first translated and then combined with representative protein sequences from the same viral genus along with *Torque teno virus 1* (NP_817122.1), an outgroup from the *Anelloviridae*, obtained from NCBI GenBank. All sequences were first aligned using MAFTT (v7.4) (Katoh and Standley, 2013) employing the E–INS–i algorithm and the alignment was trimmed using GBlocks (Talavera and Castresana, 2007; Castresana, 2000) to remove ambiguously aligned regions. Maximum likelihood phylogenetic trees were estimated in IQ-TREE (Lam-Tung et al., 2015) using the best fit amino acid model, LG, as determined by ModelFinder (Kalyaanamoorthy et al., 2017), with 1000 bootstraps replicated. Phylogenetic trees were then annotated in FigTree (http://tree.bio.ed.ac.uk/software/figtree/) and Adobe Illustrator.

4.9. Total infectome characterisation

Each sequencing library was evaluated for the presence and abundance of potential pathogenic bacterial, protozoal and fungal organisms known to potentially cause disease in avian species. Organism abundances were estimated as described above and summed for each bacterial, protozoal and fungal family/genus identified. Abundances were standardised against the number of raw reads within each sequencing library.

4.10. PCR confirmation of viral presence or absence

Primers were designed to detect and confirm amplicons of yellow-eyed penguin gyrovirus using conventional polymerase chain reaction (PCR). Primers were designed using Geneious Prime® 2022.2.1 (Biomatters Ltd.) from the complete genome of yellow-eyed penguin gyrovirus. In the Geneious® Primer Design function, four forward primers and four reverse primers were designed with each primer 18–20 bp in length with a GC content of 42.9–56.0% and a T_m of 55.1–57.9 °C. Primers were designed and selected based on identifying a product size of 620–820 bp with overlap and no repetition (Supplementary Table 2). PCR amplification was performed as follows: 15 min at 95 °C; 35 cycles of 94 °C for 30 s, 57 °C for 30 s and 72 °C for 45 s; 72 °C for 10 min. Optimisation and confirmation included utilising samples with high abundances of yellow-eyed penguin gyrovirus obtained from RNA sequencing and by altering the annealing temperature by 1 °C to maximise specificity.

PCR products were separated by gel electrophoresis with fluorophore (SYBR Safe DNA Gel Stain, Invitrogen, ThermoFisher Scientific) in a 1% agarose gel (Invitrogen, Life Technologies) on 80 mV for 35–45 min, depending on expected size and indicated quality of the PCR products,

and included negative controls, positive controls and 1 kb ladder (Invitrogen, ThermoFisher Scientific) on 0.5X TBE running buffer. PCR bands were visualised by UV light using GelDoc Go Imaging System (Bio-Rad Laboratories). Bands of the expected size were excised from the successful primers, and DNA was purified using a gel cleanup kit (Qiagen QIAquick PCR & Gel Cleanup Kit). DNA was sent for bi-directional Sanger sequencing to the University of Otago Genetic Analysis Services, New Zealand. Forward and reverse sequences were pair-end assembled using Geneious Prime®2022.2.1 software (version 11.0.14). Contigs were matched to known sequences on the NCBI database using the nt database using Basic Local Alignment Search Tool for nucleotides (BLASTn) (Altschul et al., 1990). Contigs were confirmed with the highest hit as gyrovirus. The remainder of the samples were tested individually by tissue (lung, liver, spleen, kidney and bursa) by converting RNA to cDNA using a High Capacity cDNA Reverse Transcriptase kit (Applied Biosystems, ThermoFisher Scientific) followed by PCR using YEP GV P2–F and YEP GV P2-R primers (Table 1).

4.11. Virus nomenclature

Following consultation with local iwi (indigenous peoples of Aotearoa New Zealand), we propose the virus name 'yellow-eyed penguin gyrovirus'.

Data availability

The novel yellow-eyed gyrovirus genomes can be found under GenBank accession numbers OQ064396-OQ064426. Raw sequencing reads can be found on the Aotearoa Genomic Data Repository at https://doi.org/10.57748/GG9P-8Y44.

Funding

J.R.W. was funded by the Morris Animal Foundation (MAF-D22ZO-418) and J.L.G. was funded by a New Zealand Royal Society Rutherford Discovery Fellowship (RDF-20-UOO-007).

CRediT authorship contribution statement

Janelle R. Wierenga: Conceptualization, Data curation, Formal analysis, Funding acquisition, Writing – original draft, and preparation, . **Kerri J. Morgan:** Conceptualization, Funding acquisition, Supervision, Writing – review & editing. **Stuart Hunter:** Data curation, Resources, Writing – review & editing. **Harry S. Taylor:** Resources, Writing – review & editing. **Lisa S. Argilla:** Resources, Writing – review & editing. **Trudi Webster:** Resources, Writing – review & editing. **Jeremy Dubrulle:** Data curation, Writing – review & editing. **Fátima Jorge:** Data curation, Writing – review & editing. **Mihnea Bostina:** Data curation, Resources, Writing – review & editing. **Laura Burga:** Data curation, Writing – review & editing. **Edward C. Holmes:** Writing – review & editing. **Kate McInnes:** Conceptualization, Resources, Writing – review & editing. **Jemma L. Geoghegan:** Conceptualization, Data curation, Formal analysis, Funding acquisition, Resources, Supervision, Writing – original draft, and preparation, .

Declaration of competing interest

The authors declare that they have no known competing financial interests or personal relationships that could have appeared to influence the work reported in this paper.

Acknowledgements

We would like to thank the New Zealand Department of Conservation staff, the Yellow-eyed Penguin Trust, Penguin Place, Penguin Rescue, and the Wildlife Hospital Dunedin. Thanks to Hamish Thompson for the illustration of the yellow-eyed penguin used in this manuscript. Thank you to local Kāi Tahu members for their collaboration and support.

Appendix A. Supplementary data

Supplementary data to this article can be found online at https://doi.org/10.1016/j.virol.2022.12.012.

References

Alley, M.R., Suepaul, R.B., McKinlay, B., Young, M.J., Wang, J., Morgan, K.J., et al., 2017. Diphtheritic stomatitis in yellow-eyed penguins (*Megadypyes antipodes*) in New Zealand. J. Wildl. Dis. 53 (1), 102–110.

Altschul, S.F., Gish, W., Miller, W., Myers, E.W., Lipman, D.J., 1990. Basic local alignment search tool. J. Mol. Biol. 215 (3), 403–410.

Argilla, L.S., Howe, L., Gartrell, B.D., Alley, M.R., 2013. High prevalence of Leucocytozoon spp. in the endangered yellow-eyed penguin (*Megadyptes antipodes*) in the sub-Antarctic regions of New Zealand. Parasitology 140 (5), 672–682.

Buchfink, B., Xie, C., Huson, D.H., 2015. Fast and sensitive protein alignment using DIAMOND. Nat. Methods 12 (1), 59–60.

Castresana, J., 2000. Selection of conserved blocks from multiple alignments for their use in phylogenetic analysis. Mol. Biol. Evol. 17 (4), 540–552.

Chapman, J.R., Helin, A.S., Wille, M., Atterby, C., Jarhult, J.D., Fridlund, J.S., et al., 2016. A panel of stably expressed reference genes for real-time qpcr gene expression studies of mallards (*Anas platyrhynchos*). PLoS One 11 (2).

Fang, L., Li, Y., Wang, Y., Fu, J., Cui, S., Li, X., et al., 2017. Genetic Analysis of Two Chicken Infectious Anemia Virus Variants-Related Gyrovirus in Stray Mice and Dogs: the First Report in China, 2015, vol. 2017. Biomed Research International.

Feher, E., Pazar, P., Lengyel, G., Tung Gia, P., Banyai, K., 2015. Sequence and phylogenetic analysis identifies a putative novel gyrovirus 3 genotype in ferret feces. Virus Gene. 50 (1), 137–141.

Feher, E., Bali, K., Kaszab, E., Ihasz, K., Jakab, S., Nagy, B., et al., 2022. A novel gyrovirus in a common pheasant (*Phasianus colchicus*) with poult enteritis and mortality syndrome. Arch. Virol. 167 (5), 1349–1353.

Gartrell, B., Agnew, D., Alley, M., Carpenter, T., Ha, H.J., Howe, L., et al., 2017. Investigation of a mortality cluster in wild adult yellow-eyed penguins (*Megadyptes antipodes*) at Otago Peninsula, New Zealand. Avian Pathol. 46 (3), 278–288.

Gill, J.M., Darby, J.T., 1993. Deaths in yellow-eyed penguins (*Megadyptes antipodes*) on the Otago peninsula during the summer of 1990. N. Z. Vet. J. 41 (1), 39–42.

Goldberg, T.L., Clyde, V.L., Gendron-Fitzpatrick, A., Sibley, S.D., Wallace, R., 2018. Severe neurologic disease and chick mortality in crested screamers (*Chauna torquata*) infected with a novel Gyrovirus. Virology 520, 111–115.

Goryo, M., Sugimura, H., Matsumoto, S., Umemura, T., Itakura, C., 1985. Isolation of an agent inducing chicken anemia. Avian Pathol. 14 (4), 483–496.

Goryo, M., Suwa, T., Umemura, T., Itakura, C., Yamashiro, S., 1989. Histopathology of chicks inoculated with chicken anemia agent (MSB1-TK5803 strain). Avian Pathol. 18 (1), 73–89.

Haas, B.J., Papanicolaou, A., Yassour, M., Grabherr, M., 2013. Blood PD, Bowden J, et al. De novo transcript sequence reconstruction from RNA-seq using the Trinity platform for reference generation and analysis. Nat. Protoc. 8 (8), 1494–1512.

Jeurissen, S.H.M., Wagenaar, F., Pol, J.M.A., Vandereb, A.J., Noteborn, M.H.M., 1992. Chicken anemia virus causes apoptosis of thymocytes after invivo infection and of cell-lines after invitro infection. J. Virol. 66 (12), 7383–7388.

Kalyaanamoorthy, S., Bui Quang, M., Wong, T.K.F., von Haeseler, A., Jermiin, L.S., 2017. ModelFinder: fast model selection for accurate phylogenetic estimates. Nat. Methods 14 (6), 587.

Katoh, K., Standley, D.M., 2013. MAFFT multiple sequence alignment software version 7: improvements in performance and usability. Mol. Biol. Evol. 30 (4), 772–780.

Kraberger, S., Opriessnig, T., Celer, V., Maggi, F., Okamoto, H., Blomstrom, A.-L., et al., 2021. Taxonomic updates for the genus Gyrovirus (family *Anelloviridae*): recognition of several new members and establishment of species demarcation criteria. Arch. Virol. 166 (10), 2937–2942.

Lam-Tung, N., Schmidt, H.A., von Haeseler, A., Bui Quang, M., 2015. IQ-TREE: a fast and effective stochastic algorithm for estimating maximum-likelihood phylogenies. Mol. Biol. Evol. 32 (1), 268–274.

Langmead, B., Salzberg, S.L., 2012. Fast gapped-read alignment with Bowtie 2. Nat. Methods 9 (4), 357-U54.

Li, B., Dewey, C.N., 2011. RSEM: accurate transcript quantification from RNA-Seq data with or without a reference genome. BMC Bioinf. 12.

Li, L., Pesavento, P.A., Gaynor, A.M., Duerr, R.S., Phan, T.G., Zhang, W., et al., 2015. A gyrovirus infecting a sea bird. Arch. Virol. 160 (8), 2105–2109.

Liu, Y., Lv, Q., Li, Y., Yu, Z., Huang, H., Lan, T., et al., 2022. Cross-species transmission potential of chicken anemia virus and avian gyrovirus 2. Infect. Genet. Evol. 99.

Mattern, T.M.S., Ellenberg, U., Houston, D.M., Darby, J.T., Young, M., van Heezik, Y., Seddon, P.J., 2017. Quantifying climate change impacts emphasises the importance of managing regional threats in the endangered yellow-eyed penguin. PeerJ 5, e3272.

McNulty, M.S., Connor, T.J., McNeilly, F., Spackman, D., 1989. Chicken anemia agent in the United-States - isolation of the virus and detection of antibody in broiler breeder flocks. Avian Dis. 33 (4), 691–694.

Niu, J.-T., Yi, S.-S., Dong, G.-Y., Guo, Y.-B., Zhao, Y.-L., Huang, H.-L., et al., 2019. Genomic characterization of diverse gyroviruses identified in the feces of domestic cats. Sci. Rep. 9.
Noteborn, M.H.M., Todd, D., Verschueren, C.A.J., Degauw, H., Curran, W.L., Veldkamp, S., et al., 1994. A single chicken anemia viris protein induces apoptosis. J. Virol. 68 (1), 346–351.
Phan, T.G., da Costa, A.C., Zhang, W., Pothier, P., Ambert-Balay, K., Deng, X., et al., 2015. A new gyrovirus in human feces. Virus Gene. 51 (1), 132–135.
Rosario, K., Breitbart, M., Harrach, B., Segales, J., Delwart, E., Biagini, P., et al., 2017. Revisiting the taxonomy of the family Circoviridae: establishment of the genus Cyclovirus and removal of the genus Gyrovirus. Arch. Virol. 162 (5), 1447–1463.
Smyth, J.A., Moffett, D.A., McNulty, M.S., Todd, D., Mackie, D.P., 1993. A sequential histopathological and immunocytochemical study of chicken anemia virus-infection at one-day of age. Avian Dis. 37 (2), 324–338.
Stanislawek, W.L., Howell, J., 1994. Isolation of chicken anemia virus from broiler-chickens in New-Zealand. N. Z. Vet. J. 42 (2), 58–62.
Talavera, G., Castresana, J., 2007. Improvement of phylogenies after removing divergent and ambiguously aligned blocks from protein sequence alignments. Syst. Biol. 56 (4), 564–577.
Thijl Vanstreels, R.E., Braga, E.M., Catao-Dias, J.L., 2016. Blood parasites of penguins: a critical review. Parasitology 143 (8), 931–956.
Truchado, D.A., Manuel Diaz-Piqueras, J., Gomez-Lucia, E., Domenech, A., Mila, B., Perez-Tris, J., et al., 2019. A novel and divergent gyrovirus with unusual genomic features detected in wild passerine birds from a remote rainforest in French Guiana. Viruses-Basel. 11 (12).
Urlings, H.A.P., Deboer, G.F., Vanroozelaar, D.J., Koch, G., 1993. Inactivation of chicken anemia virus in chickens by heating and fermentation. Vet. Q. 15 (3), 83–88.
Waits, K., Bradley, R.W., Warzybok, P., Kraberger, S., Fontenele, R.S., Varsani, A., 2018. Genome sequence of a gyrovirus associated with ashy storm-petrel. Microbiol. Resour. Announcem. 7 (11).
Welch, J., Bienek, C., Gomperts, E., Simmonds, P., 2006. Resistance of porcine circovirus and chicken anemia virus to virus inactivation procedures used for blood products. Transfusion 46 (11), 1951–1958.
Wuenschmann, A., Armien, A., Wallace, R., Wictor, M., Oglesbee, M., 2006. Neuronal storage disease in a group of captive Humboldt penguins (*Spheniscus humboldti*). Vet. Pathol. 43 (6), 1029–1033.
Yuasa, N., 1992. Effect of chemicals on the infectivity of chicken anemia virus. Avian Pathol. 21 (2), 315–319.
Yuasa, N., Taniguchi, T., Yoshida, I., 1979. Isolation and some characteristics of an agent inducing anemia in chicks. Avian Dis. 23 (2), 366–385.